東北大学機関リポジトリ
TOUR
Tohoku University Repository

A moment model with variable length scale for the motion of a vortex pair in two-dimensional incompressible flows

A moment model with variable length scale for the motion of a vortex pair in two-dimensional incompressible flows

Yuko Matsumoto,[a)] Kazuyuki Ueno,[b)] and Tsunenari Saito
Department of Aerospace Engineering, Tohoku University, Sendai 980-8759, Japan

A simple model for the motion of a vortex pair in two-dimensional inviscid flows is presented. In this model the motion of the vortex pair is expressed by a set of ordinary differential equations for the dipole moment, the length scale, and the centroid position. The length scale is the distance between the positive vortex and the negative vortex in the pair. A self-propelling velocity of the model vortex pair is introduced in response to a wide range of the length scale. If a background flow is a linear function of the position, the dipole moment and the length scale of the model are exact. This model works well for a separated vortex pair, although it is not applicable to an asymmetrically deformed vortex pair. © 2009 *American Institute of Physics*. [DOI: 10.1063/1.3118648]

I. INTRODUCTION

A dipolar vortex is one of the basic vortical structures of two-dimensional flows. It contains a pair of equal and opposite vortices, and has often been observed in the atmosphere[1] and oceans.[2] A dipolar vortex has a self-propelling motion which can transport fluid mass, momentum, and heat. Therefore, it is important to understand how background flows affect the motion of a dipolar vortex.

A numerical study by Kida *et al.*[3] showed that a dipolar vortex was deformed into a head-tail structure in a cooperative strain flow. Trieling *et al.*[4] confirmed experimentally the prediction of Kida *et al.* Furthermore, Trieling *et al.* studied, both numerically and experimentally, the motion of a dipolar vortex separated by an adverse strain flow. On the other hand, models for the motion of a dipolar vortex on the β-plane were developed by Hobson[5] and Shivamoggi and van Heijst.[6] However, studies of a dipole in other background flows are less common in literature.

In this paper, the motion of a vortex pair consisting of two contour-rotating vortices of finite area in a steady background flow is studied through a simple model. In this model, the evolution of the vortex pair is governed by a set of ordinary differential equations for the dipole moment, the dipole position, and the length scale. The motion of a vortex pair in various background flows is calculated by the present model and the validity of the model is discussed by comparing to corresponding solutions of the vortex method.

II. DIPOLE MOMENT OF A VORTEX PAIR

The motion of a vortex pair in a two-dimensional incompressible inviscid flow in an unbounded domain is considered in the present study. A schematic of the vortex pair is shown in Fig. 1. The vortex pair consists of equal and opposite vortices of finite area. Positive vorticity and negative vorticity fill regions Ω_+ and Ω_-, respectively. Then circulation Γ is given by the following area integral of the vorticity ω,

$$\Gamma = \int_{\Omega_+} \omega(\boldsymbol{x})dS = -\int_{\Omega_-} \omega(\boldsymbol{x})dS. \tag{1}$$

The area of vortices S is given by

$$S = \int_{\Omega} dS, \tag{2}$$

where the domain of integration is $\Omega = \Omega_+ + \Omega_-$. The circulation and the area are constant because the flow is inviscid and incompressible.

The centroid of the vortex pair $\boldsymbol{x}_d$ is defined as the midpoint between centroids of positive vortex $\boldsymbol{x}_+$ and negative vortex $\boldsymbol{x}_-$,

$$\boldsymbol{x}_{\pm} = \pm \frac{1}{\Gamma} \int_{\Omega_{\pm}} \boldsymbol{x}\omega(\boldsymbol{x})dS, \tag{3}$$

$$\boldsymbol{x}_d = (\boldsymbol{x}_+ + \boldsymbol{x}_-)/2. \tag{4}$$

The following length scale a is introduced in this study:

$$a = |\boldsymbol{x}_+ - \boldsymbol{x}_-|. \tag{5}$$

This variable, which shows the distance between the positive vortex and the negative vortex in the pair, plays an important role in this study.

A flow field induced by the vortex pair is expressed in terms of a stream function ψ_d as

$$\psi_d(\boldsymbol{x}) = -\frac{1}{2\pi} \int_{\Omega} \omega(\boldsymbol{x}')\log|\boldsymbol{x} - \boldsymbol{x}'|dS'. \tag{6}$$

The assumption that $\boldsymbol{x}$ is far from the vortex pair gives

---

a)Electronic mail: y-mats@cfd.mech.tohoku.ac.jp.
b)Electronic mail: ueno@cfd.mech.tohoku.ac.jp.

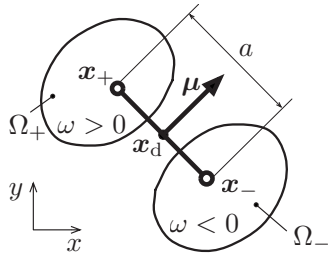FIG. 1. Schematic of a vortex pair. The region and the centroid of each vortex are denoted by $\Omega_\pm$ and $\boldsymbol{x}_\pm$, respectively. The arrow shows the dipole moment $\boldsymbol{\mu}$. The centroid and the length scale of the vortex pair are denoted by $\boldsymbol{x}_d$ and a.

$$\log|(\boldsymbol{x}-\boldsymbol{x}_d)-(\boldsymbol{x}'-\boldsymbol{x}_d)| = \log r - \frac{(\boldsymbol{x}-\boldsymbol{x}_d)\cdot(\boldsymbol{x}'-\boldsymbol{x}_d)}{r^2}$$
$$+ O\left[\left(\frac{r'}{r}\right)^2\right], \tag{7}$$

where $r=|\boldsymbol{x}-\boldsymbol{x}_d|$ and $r'=|\boldsymbol{x}'-\boldsymbol{x}_d|$. Substituting Eq. (7) into Eq. (6) yields

$$\psi_d(\boldsymbol{x}) = \frac{1}{2\pi r^2}\boldsymbol{\mu}\times(\boldsymbol{x}-\boldsymbol{x}_d)\cdot\boldsymbol{e}_z + O\left[\left(\frac{r'}{r}\right)^2\right]\Gamma, \tag{8}$$

where $\boldsymbol{e}_z$ is the unit vector in the z-direction and $\boldsymbol{\mu}$ is the first-order moment of vorticity defined by

$$\boldsymbol{\mu} = \int_\Omega (\boldsymbol{x}'-\boldsymbol{x}_d)\omega(\boldsymbol{x}')dS' \times \boldsymbol{e}_z. \tag{9}$$

If the second term of the right-hand side of Eq. (8) is negligibly small, Eq. (8) is reduced to the flow field induced by a point dipole at $\boldsymbol{x}_d$ with the dipole moment $\boldsymbol{\mu}$. Definition (9) is applicable to a finite area vortex pair in any shape, and the dipole moment characterizes the direction and the strength of the vortex pair.

III. FORMULATION OF THE MOMENT MODEL

In the present study, a moment model[7] for a vortex pair in connection with the dipole moment is proposed. In this moment model, the vortex pair is represented by three variables and two constants: the centroid $\boldsymbol{x}_d(t)$, the length scale $a(t)$, and the dipole moment $\boldsymbol{\mu}(t)$ are the variables; the circulation Γ and the area S are the constants. The motion of the vortex pair in a background flow is described by a set of time evolution equations for the above three variables. The derivations of the evolution equations for the variables of the moment model are described in this section.

First, let us consider the length scale. Substituting Eq. (3) into Eq. (9) yields the following relation between the length scale and the dipole moment:

$$a(t) = \mu(t)/\Gamma, \tag{10}$$

where $\mu=|\boldsymbol{\mu}|$. According to Kelvin's circulation theorem, the circulation around a material circuit in an inviscid fluid is invariant with respect to the fluid motion. Therefore, the circulation $\pm\Gamma$ of each vortex is conserved during the vortex pair evolution. Consequently, the length scale $a(t)$ varies in

proportion to the magnitude of the dipole moment $\mu(t)$.

Next, the evolution equation for the centroid $\boldsymbol{x}_d$ of the vortex pair is discussed. It is expressed as

$$\frac{d\boldsymbol{x}_d}{dt} = \boldsymbol{U}(\boldsymbol{x}_d) + \boldsymbol{u}_{\text{self}}(t), \tag{11}$$

where $\boldsymbol{U}(\boldsymbol{x}_d)$ is the velocity of the background flow at $\boldsymbol{x}=\boldsymbol{x}_d$, and $\boldsymbol{u}_{\text{self}}$ is the self-propelling velocity of the vortex pair. In a fluid at rest the vortex pair moves with $\boldsymbol{u}_{\text{self}}$ parallel to the dipole moment. This is not the same as the velocity $\nabla\times(\psi_d\boldsymbol{e}_z)|_{\boldsymbol{x}_d}$ induced by the vortex pair at its own centroid. When the two vortices in the pair are far apart from each other, the self-propelling velocity is approximately given as follows:[8]

$$u_{\text{self}} = |\boldsymbol{u}_{\text{self}}| = \frac{\Gamma}{2\pi a}. \tag{12}$$

Unfortunately, Eq. (12) is inadequate when the vortices are close to each other.[8] If the vortices are in touch each other and Ω is a circle of radius R, the self-propelling velocity is given by

$$u_{\text{self}} = \frac{\mu}{2\pi R^2}, \tag{13}$$

where R is a constant equal to $\sqrt{S/\pi}$. The flow field induced by this circular vortex pair outside of Ω is equivalent to the flow field induced by a circular cylinder of radius R moving at the same speed with Eq. (13).[9] The self-propelling velocity should smoothly vary with $a(t)$ between Eqs. (12) and (13). Let $u_{\text{self}}=\Gamma a/(k_1 a^2 + k_2 aR + k_3 R^2)$, where k_i is a constant coefficient. On the assumptions that u_{self} satisfies conditions given by Eq. (12) for $a\gg C_0 R$ and Eq. (13) for $a=C_0 R$, the following expression is introduced in this study:

$$u_{\text{self}} = \frac{\Gamma}{2\pi}\frac{4C_0 a}{(a-C_0 R)(4C_0 a - R) + 4aR}, \tag{14}$$

where the constant C_0 is the value of a/R when Ω is a circle.

Finally, the evolution equation for the dipole moment is derived. Let us consider the conservation of momentum of the fluid around the vortex pair in the Lagrangian frame which moves at the same velocity as the vortex pair. A control volume V_c encloses the vortex pair with a certain margin. The conservation of momentum is expressed as

$$\frac{d}{dt}\int_{V_c}\rho\boldsymbol{u}\,dV + \int_{S_c}\rho\boldsymbol{u}\left(\boldsymbol{u}-\frac{d\boldsymbol{x}_d}{dt}\right)\cdot\boldsymbol{n}\,dS = -\int_{S_c}p\boldsymbol{n}\,dS, \tag{15}$$

where $\boldsymbol{u}$ is the velocity, p is the pressure, ρ is the density of the flow field, and $\boldsymbol{n}$ is the unit vector normal to the control surface S_c. Here, the velocity $\boldsymbol{u}$ is decomposed into the background flow $\boldsymbol{U}$ and the induced flow by the vortex pair $\nabla\times(\psi_d\boldsymbol{e}_z)$,

$$\boldsymbol{u} = \boldsymbol{U}(\boldsymbol{x}) + \nabla\times[\psi_d(\boldsymbol{x},t)\boldsymbol{e}_z]. \tag{16}$$

The background flow $\boldsymbol{U}(\boldsymbol{x})$ is expanded about $\boldsymbol{x}_d(t)$ as

$$U(x) = U(x_d) + (x - x_d) \left.\frac{\partial U}{\partial x}\right|_{x_d} + (y - y_d) \left.\frac{\partial U}{\partial y}\right|_{x_d} + \cdots .$$

(17)

In order to obtain the pressure using the velocity, it is assumed that the background flow U is a flow field of constant vorticity ω_c. Since the flow field induced by the vortex pair $\nabla \times (\psi_d e_z)$ is irrotational on the control surface S_c, the pressure is obtained from Bernoulli's equation for the region of constant vorticity[8,9] as follows:

$$\frac{p}{\rho} = -\frac{\partial \phi}{\partial t} - \frac{1}{2}u^2 - \omega_c \psi + F(t),$$

(18)

where ϕ is the velocity potential of the irrotational part of u, ψ is the stream function of Eq. (16), and $F(t)$ is an arbitrary function of time. Substituting Eqs. (8) and (16)–(18) into Eq. (15) and integrating it, evolution equation for the dipole moment is obtained as follows:

$$\frac{d\mu_x}{dt} = -\mu_x \left.\frac{\partial U}{\partial x}\right|_{x_d} - \mu_y \left.\frac{\partial V}{\partial x}\right|_{x_d},$$

$$\frac{d\mu_y}{dt} = -\mu_x \left.\frac{\partial U}{\partial y}\right|_{x_d} - \mu_y \left.\frac{\partial V}{\partial y}\right|_{x_d}.$$

(19)

These equations are of the same form as the equation derived from relation (10) by Winckelmans[10] and the equations obtained by Roberts[11] and Buttke[12] in terms of a Hamiltonian for the incompressible Euler equations. Equation (19) is exact if the Taylor series (17) of the background flow does not have the higher-order terms. It is also exact if the induced flow field (6) by the vortex pair does not have the higher-order moment. Contribution of the higher-order terms to evolution of μ when both ψ_d and U include the higher-order terms are neglected in Eq. (19). Equations (10), (11), (14), and (19) constitute the moment model for motion of the vortex pair.

IV. BEHAVIOR OF THE VORTEX PAIR IN LINEAR BACKGROUND FLOWS

If a background velocity field U is a linear function of the coordinates x and y, the evolution equation for the dipole moment (19) has no modeling error. Therefore, the solution of Eq. (19) represents the dipole moment of an actual vortex pair in the linear background flow, and it can be obtained analytically. Behavior of such vortex pairs in the linear background flows is investigated in this section.

Let us consider the linear background flow given by the following stream function:

$$\Psi = \frac{A}{2}x^2 + \frac{1}{2}y^2.$$

(20)

Streamlines of Eq. (20) are shown in Fig. 2. Our attention is restricted to the cases when $|A| \le 1$. The other cases when $|A| > 1$ or when Eq. (20) has a term of xy with nonzero coefficient are omitted here because flow fields for such cases are obtained by the coordinate rotation of Eq. (20) around the z-axis.
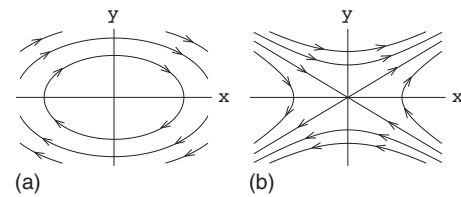

FIG. 2. Streamlines of linear background flows given by $\Psi = (Ax^2 + y^2)/2$. (a) $A = 0.36$. (b) $A = -0.36$.

For intuitive understanding of behavior of the vortex pair, the angle of the dipole moment $\beta = \tan^{-1}(\mu_y/\mu_x)$ and the length scale $a = \mu/\Gamma$ are used instead of the Cartesian components μ_x and μ_y in the following part of this section, although analytic solutions of μ_x and μ_y are obtained (see Appendix). Equations for β and a are derived from Eqs. (10), (19), and (20) as follows:

$$\frac{d\beta}{dt} = -\cos^2 \beta - A \sin^2 \beta,$$

(21)

$$\frac{1}{a}\frac{da}{dt} = -(1 - A)\sin \beta \cos \beta.$$

(22)

The vortex pair rotates anticlockwise if $d\beta/dt > 0$, and clockwise if $d\beta/dt < 0$. The distance between two vortices in the pair increases if $da/dt > 0$ and decreases if $da/dt < 0$. The right-hand sides of Eqs. (21) and (22) show that the evolution of β and a does not depend on the position x_d at all. Indeed, these equations are solved analytically and the solutions are obtained as

$$\beta(t) = -\tan^{-1}\left[\frac{\tan\{\sqrt{A}t - \tan^{-1}(\sqrt{A}\tan \beta_0)\}}{\sqrt{A}}\right],$$

(23)

$$a(t) = a_0 \sqrt{\frac{-1 - A + (-1 + A)\cos 2\beta_0}{-1 - A + (-1 + A)\cos 2\beta(t)}},$$

(24)

where a_0 and β_0 denote initial values of a and β, respectively. Evolution of the length scale a depends on only the initial angle β_0 and the parameter A of the background flow. Further, the following relation between β and a is obtained by dividing Eq. (22) by Eq. (21):

$$\frac{1}{a}\frac{da}{d\beta} = \frac{(1 - A)\sin \beta \cos \beta}{\cos^2 \beta + A \sin^2 \beta}.$$

(25)

If $A = 0$, the background flow is a shear flow parallel to the x-axis. In this case, the angular rate $d\beta/dt$ is negative except when $\beta = \pi/2$ and $3\pi/2$. Thus, the vortex pair rotates clockwise, and then, the moment gradually approaches a direction parallel to the y-axis. This means that the two vortices in the pair are horizontally aligned. Because the right-hand side of Eq. (22) is $-\sin \beta \cos \beta$, the growth rate da/dt is negative for $0 < \beta < \pi/2$ or $\pi < \beta < 3\pi/2$, while positive for the other β (see Fig. 3). This relation between β and da/dt is common to all cases for $|A| < 1$. In addition, it is found from Eq. (25) that the length scale has a local minimum $a/a_0 = |\cos \beta_0|$ at $\beta = 0$ or π. The evolution of β and a for various initial angle β_0 is summarized in Table I. For
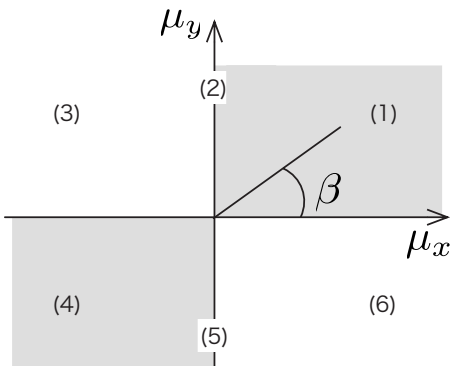
FIG. 3. Ranges of β for $da/dt < 0$ (shaded area) in the shear flow $\Psi = y^2/2(A=0)$. The numbers in this figure correspond to those in Table I.

FIG. 4. Ranges of β for $da/dt < 0$ (shaded area) in the strain flow $\Psi = (Ax^2 + y^2)/2$ for $-1 \leq A < 0$. The numbers in this figure correspond to those in Table II.

example, in the case of $\pi < \beta_0 < 3\pi/2$ [region (4) in Fig. 3], the vortex pair rotates clockwise and the length scale initially decreases. The length scale takes the minimum value at $\beta = \pi$. Thereafter, the vortex pair continues to rotate clockwise while the length scale increases. On the other hand, in the case of $\pi/2 < \beta_0 \leq \pi$ [region (3) in Fig. 3], the length scale monotonically increases. At the final stage of the evolution, the direction of the vortex pair approaches $\beta \to \pi/2$ [axis (2) in Fig. 3] and the length scale continues to increase in proportion to time for any case of $\pi/2 < \beta_0 < 3\pi/2$.

If $0 < A < 1$, streamlines of the background flow (20) are elliptic curves, as shown in Fig. 2(a). In this case, Eq. (21) gives $d\beta/dt < 0$ for all β. Hence, the vortex pair always rotates clockwise. Equation (25) for $0 < A < 1$ implies that a periodically changes with β, and a has the following minimum value at $\beta = 0$ or π and the following maximum value at $\beta = \pi/2$ or $3\pi/2$:

$$\sqrt{A \sin^2 \beta_0 + \cos^2 \beta_0} \leq \frac{a}{a_0} \leq \sqrt{\sin^2 \beta_0 + (\cos^2 \beta_0)/A}.$$

$$(26)$$

The length scale a is always larger than the initial value a_0 if $\beta_0 = 0$ or π and always smaller than a_0 if $\beta_0 = \pi/2$ or $3\pi/2$.

In case of $A=1$, the background flow velocity is the same as the velocity of a rigid-body rotation. In this flow, a is a constant and $d\beta/dt$ is the same constant as the angular rate of the rotating background flow.
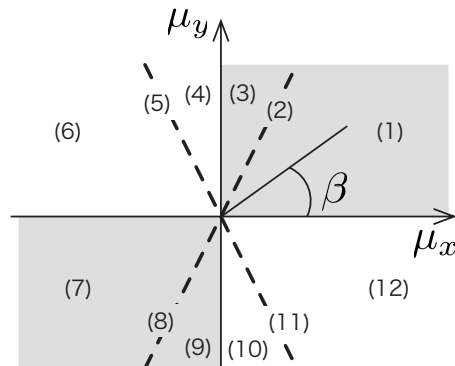
If $-1 \leq A < 0$, background (20) is a strain flow with a constant vorticity $\omega_c = -(1-|A|)$, as shown in Fig. 2(b). In contrast with the cases of $0 \leq A \leq 1$, the sign of $d\beta/dt$ for $-1 \leq A < 0$ depends on β: the angular rate $d\beta/dt$ is positive when $\tan^2 \beta > 1/|A|$, while negative when $\tan^2 \beta < 1/|A|$. The vortex pair rotates to approach $\beta \to \pi - \tan^{-1}\sqrt{1/|A|}$ or $2\pi - \tan^{-1}\sqrt{1/|A|}$ without change in rotational direction, although the vortex pair keeps its initial direction if $\tan \beta_0 = \pm \sqrt{1/|A|}$. The length scale a decreases if $0 < \beta < \pi/2$ or $\pi < \beta < 3\pi/2$ and increases if $\pi/2 < \beta < \pi$ or $3\pi/2 < \beta < 2\pi$ (see Fig. 4). Equation (25) gives a local minimum of the length scale $a/a_0 = \sqrt{\cos^2 \beta_0 - |A|\sin^2 \beta_0}$ at $\beta = 0$ or π, and another local minimum $a/a_0 = \sqrt{\sin^2 \beta_0 - (\cos^2 \beta_0)/|A|}$ at $\beta = \pi/2$ or $3\pi/2$. The evolution of β and a for various initial angle β_0 is summarized in Table II. For example, if $\pi < \beta_0 < \pi + \tan^{-1}\sqrt{1/|A|}$ [region (7) in Fig. 4], the vortex pair rotates clockwise and a decreases to the minimum value at $\beta = \pi$. Thereafter, the pair continues to rotate while a increases. On the other hand, if $\pi - \tan^{-1}\sqrt{1/|A|} < \beta_0 \leq \pi$ [region (6) in Fig. 4], the length scale monotonically increases with clockwise rotation. At the final stage of the evolution, the direction of the vortex pair approaches $\beta \to \pi - \tan^{-1}\sqrt{1/|A|}$ [axis (5) in Fig. 4], and the length scale continues to increase exponentially with time for any case of $\pi - \tan^{-1}\sqrt{1/|A|} < \beta_0 < \pi + \tan^{-1}\sqrt{1/|A|}$. In other instances, if $\beta_0 = \pi + \tan^{-1}\sqrt{1/|A|}$ or $\pi - \tan^{-1}\sqrt{1/|A|}$, the angle β keeps constant, while a exponentially decreases or increases, respectively. The exponen-

TABLE I. Behavior of a vortex pair in the shear flow $\Psi = y^2/2$ ($A=0$).

No.	β_0	$d\beta/dt$	$\lim_{t \to \infty} \beta$	Evolution of the length scale a/a_0
(1)	$0 < \beta_0 < \pi/2$	Negative	$3\pi/2$	Decrease to the minimum value $\|\cos \beta_0\|$ at $\beta=0$, thereafter increase
(2)	$\pi/2$	0	$\pi/2$	Constant
(3)	$\pi/2 < \beta_0 \leq \pi$	Negative	$\pi/2$	Monotonic increase
(4)	$\pi < \beta_0 < 3\pi/2$	Negative	$\pi/2$	Decrease to the minimum value $\|\cos \beta_0\|$ at $\beta=\pi$, thereafter increase
(5)	$3\pi/2$	0	$3\pi/2$	Constant
(6)	$3\pi/2 < \beta_0 \leq 2\pi$	Negative	$3\pi/2$	Monotonic increase

TABLE II. Behavior of a vortex pair in the strain flow $\Psi=(Ax^2+y^2)/2$ for $-1\le A<0$. The constant β_A in this table denotes $\tan^{-1}\sqrt{1/|A|}$.

No.	β_0	$d\beta/dt$	$\lim_{t\to\infty}\beta$	Evolution of the length scale a/a_0
(1)	$0<\beta_0<\beta_A$	Negative	$2\pi-\beta_A$	Decrease to $\sqrt{\cos^2\beta_0-|A|\sin^2\beta_0}$ at $\beta=0$, thereafter increase
(2)	β_A	0	β_A	Exponential decrease
(3)	$\beta_A<\beta_0<\pi/2$	Positive	$\pi-\beta_A$	Decrease to $\sqrt{\sin^2\beta_0-(\cos^2\beta_0)/|A|}$ at $\beta=\pi/2$, thereafter increase
(4)	$\pi/2\le\beta_0<\pi-\beta_A$	Positive	$\pi-\beta_A$	Monotonic increase
(5)	$\pi-\beta_A$	0	$\pi-\beta_A$	Exponential increase
(6)	$\pi-\beta_A<\beta_0\le\pi$	Negative	$\pi-\beta_A$	Monotonic increase
(7)	$\pi<\beta_0<\pi+\beta_A$	Negative	$\pi-\beta_A$	Decrease to $\sqrt{\cos^2\beta_0-|A|\sin^2\beta_0}$ at $\beta=\pi$, thereafter increase
(8)	$\pi+\beta_A$	0	$\pi+\beta_A$	Exponential decrease
(9)	$\pi+\beta_A<\beta_0<3\pi/2$	Positive	$2\pi-\beta_A$	Decrease to $\sqrt{\sin^2\beta_0-(\cos^2\beta_0)/|A|}$ at $\beta=3\pi/2$, thereafter increase
(10)	$3\pi/2\le\beta_0<2\pi-\beta_A$	Positive	$2\pi-\beta_A$	Monotonic increase
(11)	$2\pi-\beta_A$	0	$2\pi-\beta_A$	Exponential increase
(12)	$2\pi-\beta_A<\beta_0\le2\pi$	Negative	$2\pi-\beta_A$	Monotonic increase

tial increase in a at $\beta=\pi-\tan^{-1}\sqrt{1/|A|}$ is caused by the characteristics of the background flow, and there is no physical inconsistency.

Equations and solutions for the length scale a and the angle of the dipole moment β are exact in the linear background flow as mentioned before. Therefore the validity of the system of the moment model in the linear background flow depends on the modeling of $d\mathbf{x}_d/dt$, that is, the approximation of the self-propelling speed u_{self}.

The self-propelling speed u_{self} introduced in Eq. (14) is proposed so as to be applicable to vortex pairs in a wide range of a, although its validity has not been confirmed yet. Therefore, the validity of Eq. (14) is discussed in Sec. V in comparison between numerical simulations by the moment model and the vortex method.

The self-propelling speed u_{self} given by Eq. (14) is introduced on the assumption that the vortex pair is symmetric. However, there is a possibility that the actual vortex pair is asymmetrically deformed and broken up into three or more vortices by the background flow and a vortex-vortex interac-

tion. The moment model has no information on such internal deformation, and it is probably not applicable to the broken vortex pair. Therefore, the range of application of the moment model should be clarified in comparison with behavior of actual vortex pairs in various background flows.

V. VALIDATION OF THE MOMENT MODEL BY NUMERICAL SIMULATIONS

In this section, time evolutions of a vortex pair in several types of background flows are calculated by the moment model. In order to show the validity of the moment model, the results of the model are compared to the numerical results of the equivalent vortex pair calculated by the vortex method.[13] The vortex method gives reliable solution for two-dimensional Euler equations when there is no boundaries and the number of vortex elements are sufficient.

In moment model calculations, motions of a vortex pair are obtained by solving the system of Eqs. (10) and (11) with Eq. (14), and Eq. (19) numerically. The value of the coeffi-
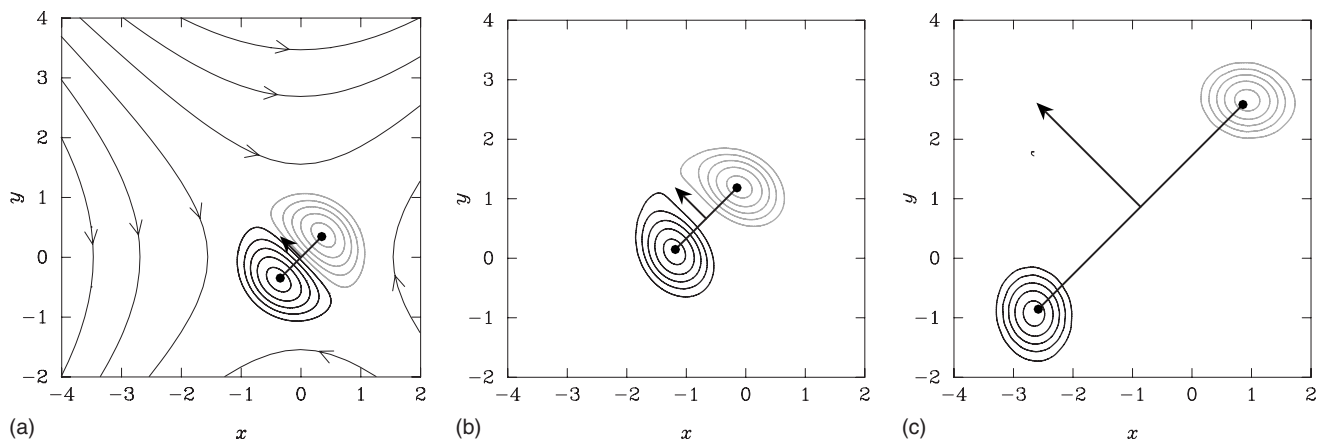

FIG. 5. Evolution of a vortex pair in the adverse strain flow $\Psi=(-x^2+y^2)/2$. The arrow indicates the dipole moment $\boldsymbol{\mu}$, and the line segment perpendicular to the arrow shows the length scale a of the moment model. Contours show vorticity calculated by the vortex method. Streamlines of the background strain flow are shown in (a). The initial conditions of the vortex pair are $\mathbf{x}_d=(0,0)$, $\mu=25.5415$, $\beta_0=3\pi/4$, and $a_0=1.0216$ ($R=\pi/\sqrt{8}$ and $\Gamma=25$). (a) $t=0$, (b) $t=0.4$, and (c) $t=1.6$.
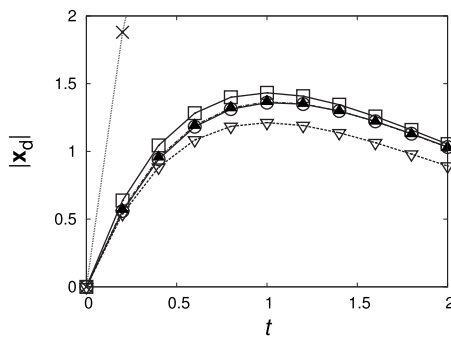
FIG. 6. Position of the vortex pair centroid in the adverse strain flow displayed in Fig. 5. The centroid is calculated by the moment model and the vortex method (solid triangles). Profiles for the moment model are calculated using Eqs. (12) (squares), (13) (inverted open triangles), and (14) (circles) as the self-propelling speed, and evolution equation $dx_d/dt = u(x_d)$ (crosses).

cient $C_0 = a_0/R$ in Eq. (14) is fixed at 0.9198 after the Lamb–Chaplygin dipole. The forth-order Runge–Kutta method is used for time integration with $\Delta t = 10^{-4} - 10^{-3}$.

In the vortex method, the vorticity field is discretized by thousands of vortex elements and the evolution of elements is obtained from the vorticity equation in the Lagrangian description. For smoothness and accuracy, the Gaussian kernel is used as a cutoff function. The second-order Adams–Bashforth scheme is used for time integration with $\Delta t = (1 \times 10^{-3}) - (5 \times 10^{-3})$. An initial condition for the vortex pair is given by the Lamb–Chaplygin dipole,[9,14] which is equivalent to the initial condition of the moment model. After obtaining the results of the vortex method, the centroid position, the length scale, and the dipole moment are calculated from the vorticity distribution by using Eqs. (4), (5), and (9), respectively.

A. Motion of a vortex pair in a strain flow

Let us consider a vortex pair in the strain flow obtained by Eq. (20) with $A = -1$ in order to validate u_{self} given by Eq. (14). Two initial cases corresponding to Table II [(5) and (2)] are calculated; $\beta_0 = 3\pi/4$ and $\pi/4$. For these cases solutions (23) and (24) are simplified to

$$\beta(t) = \beta_0, \tag{27}$$

$$a(t) = \begin{cases} a_0 e^t, & (\beta_0 = 3\pi/4) \\ a_0 e^{-t}, & (\beta_0 = \pi/4). \end{cases} \tag{28}$$

The distance between vortices exponentially increases if $\beta_0 = 3\pi/4$ and exponentially decreases if $\beta_0 = \pi/4$ without rotation. Initial configurations of the vortex pair are illustrated in Figs. 5(a) and 7(a). In terms of effect of the strain flow on the vortex pair motion, the former case is referred to as "adverse" and the latter is referred to as "cooperative" after Trieling et al.[4] In both cases, initial values of the centroid, the length scale, and the dipole moment are given by $x_d = 0$, $a_0 = C_0 R = 1.0216$, and $\mu = a_0 \Gamma = 25.5415$, where $R = \pi/\sqrt{8}$ and $\Gamma = 25$. The value of R and the initial ratio u_{self}/U are the same as those used by Kida et al.[3]

Figure 5 shows results for the adverse case corresponding to Table II (5). In this figure and other similar figures shown later, the results of the moment model and the vortex method are plotted together. The thick arrow indicates the dipole moment vector $\boldsymbol{\mu}$ and the thick line segment perpendicular to the arrow shows the length scale a of the moment model. The intersection point of the dipole moment vector with the line segment of the length scale indicates the centroid of the vortex pair calculated by the moment model. The thin lines indicate contours of vorticity calculated by the vortex method. Black lines illustrate contours of positive vorticity and gray lines illustrate contours of negative vorticity. The contour levels are 10%, 30%, 50%, 70%, and 90% of the initial maximum or minimum of vorticity. Streamlines of the background flow are also displayed by thin lines in the figures at $t = 0$.

Vorticity contours in Fig. 5 show that two vortices separate with time and the shape of each vortex approaches a circle. This behavior agrees with the experimental and numerical study by Trieling et al.[4] The length scale of the moment model increases as described in Eq. (28) corresponding to the separation of vortices obtained by the vortex method. The centroid position $|x_d|$ versus time is shown in Fig. 6. In order to show the advantage of u_{self} given by Eq. (14), profiles using u_{self} given by Eqs. (12) and (13) are also plotted.
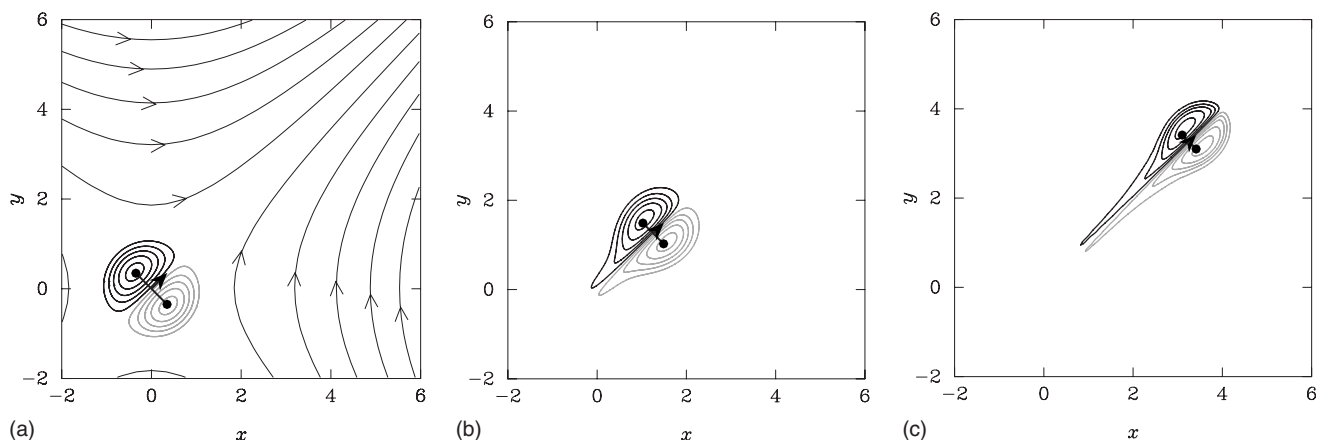

FIG. 7. Evolution of a vortex pair in the cooperative strain flow $\Psi = (-x^2 + y^2)/2$. The initial conditions are $x_d = (0,0)$, $\mu = 25.5415$, $\beta_0 = \pi/4$, and $a_0 = 1.0216$ ($R = \pi/\sqrt{8}$ and $\Gamma = 25$). (a) $t = 0$, (b) $t = 0.4$, and (c) $t = 0.8$.
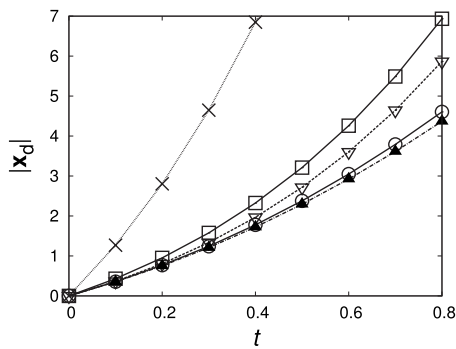
FIG. 8. Position of the vortex pair centroid in the cooperative strain flow shown in Fig. 7. The centroid is calculated by the moment model and the vortex method. Meanings of symbols are the same as Fig. 6.
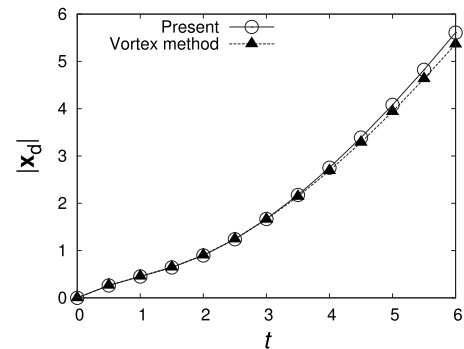

FIG. 10. Position of the vortex pair centroid in the shear flow shown in Fig. 9. The centroid is calculated by the moment model and the vortex method.

In addition, a profile using the incorrect relation $d\boldsymbol{x}_d/dt = \boldsymbol{u}(\boldsymbol{x}_d)$ is also plotted. The result using u_{self} given by Eq. (14) is in good agreement with the result of the vortex method in comparison with Eqs. (12) and (13) and $d\boldsymbol{x}_d/dt=\boldsymbol{u}(\boldsymbol{x}_d)$ in this case.

Next, let us consider the cooperative strain flow corresponding to Table II (2) in which the distance between two vortices in the pair decreases (Fig. 7). Vorticity contours calculated by the vortex method show that this strain flow elongates the vortex pair in the direction of the dipole moment. This elongated "tail" is observed at the rear side after $t=0.4$, as shown in Figs. 7(b) and 7(c). This deformed vortex pair is referred to as a "head-tail structure."[3,4] The length scale obtained by the moment model decreases as described in Eq. (28) and agrees very well with the result of the vortex method because the background flow is linear. The centroid position $|\boldsymbol{x}_d|$ versus time is shown in Fig. 8. The result using u_{self} given by Eq. (14) is the best approximation of the result of the vortex method in comparison with Eqs. (12) and (13) and $d\boldsymbol{x}_d/dt=\boldsymbol{u}(\boldsymbol{x}_d)$ in this case. As far as our many test calculations including the above results show, Eq. (14) gives a good approximation for u_{self} if the length scale changes without rotation.

B. Motion of a vortex pair in shear flows

In the last subsection, the validity of Eq. (14) in the cases without rotation of a vortex pair has been shown. Here, let us consider cases in which both the direction and the length scale of the vortex pair change with time, and investigate a relation between deformation of the vortex pair and the range of application of the moment model. As typical cases with rotation in linear background flows, motions of the vortex pair in the shear flow described in Table I [(3) and (1)] are illustrated. Initial configurations of the vortex pair are shown in Figs. 9(a) and 11(a). Initial conditions are set to $\boldsymbol{x}_d=(0,0)$, $\mu=1$, $a_0=0.4599(R=0.5)$, and $\beta_0=3\pi/4$ or $\pi/4$.

Figure 9 shows results of the moment model and the vortex method in the case of $\beta_0=3\pi/4$, in which the distance between vortices in the pair monotonically increases and the vortex pair rotates clockwise. Vorticity contours obtained by the vortex method show that the shape of each vortex in the pair approaches a circle with increasing their distance, and the symmetry of two vortices is preserved even when the vortex pair is rotated by this background flow. Figure 10 shows time profiles of the centroid position $|\boldsymbol{x}_d|$ of the vortex pair depicted in Fig. 9. A good agreement is observed between the present model and the vortex method. As far as our many test calculations in linear back ground flows including the above result show, the symmetry of separated vortex
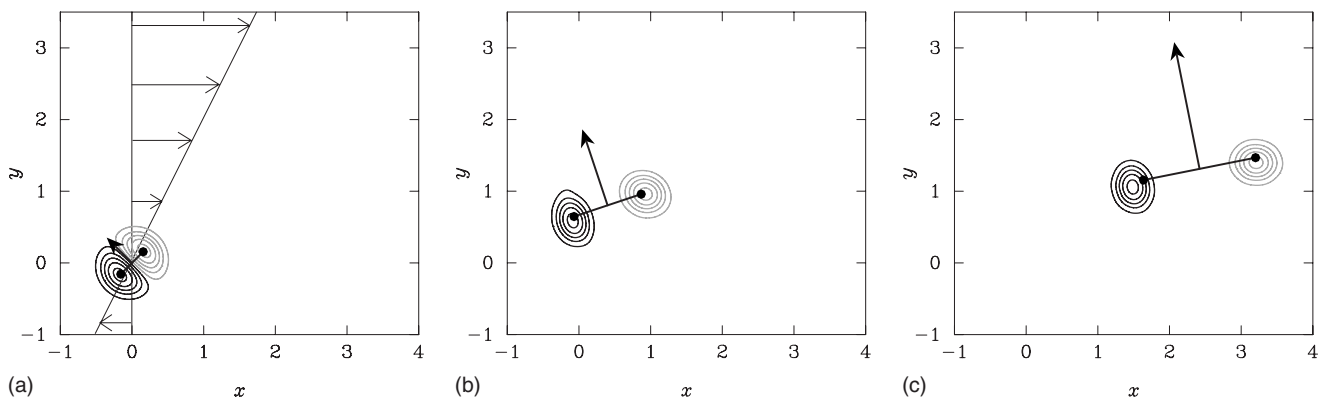

FIG. 9. Evolution of a vortex pair in the shear flow $\Psi=y^2/2$. The initial conditions for the vortex pair are $\boldsymbol{x}_d=(0,0)$, $\mu=1$, $\beta_0=4\pi/3$, and $a_0=0.4599(R=0.5)$. Velocity vectors of the shear flow are shown in (a). (a) $t=0$, (b) $t=2$, and (c) $t=4$.
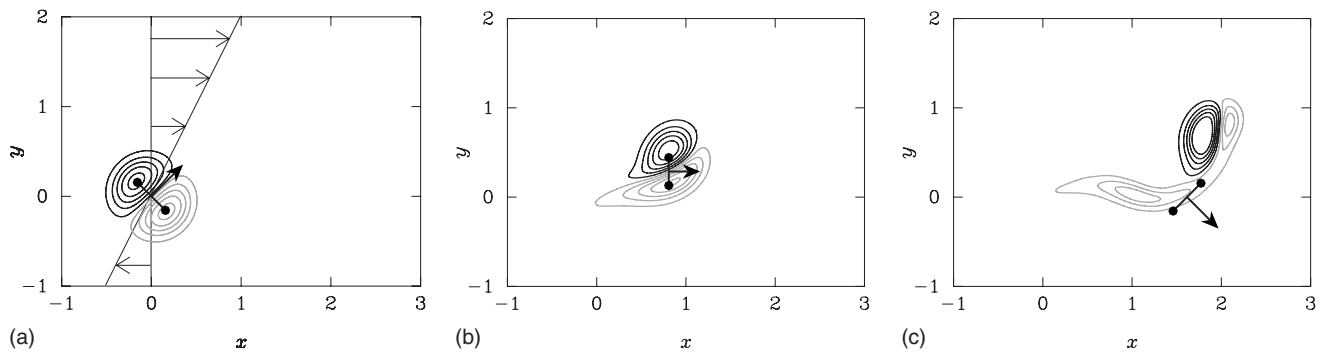
FIG. 11. Evolution of a vortex pair in the shear flow $\Psi = y^2/2$. The initial conditions for the vortex pair are $x_d = (0,0)$, $\mu = 1$, $\beta_0 = \pi/4$, and $a_0 = 0.4599(R = 0.5)$. (a) $t = 0$, (b) $t = 1$, and (c) $t = 2$.

pairs for $a(t) > a_0(=C_0 R)$ are preserved. In such cases, Eq. (14) of the moment model gives a good approximation for u_{self} even when the vortex pair rotates.

Figure 11 shows results in the case of $\beta_0 = \pi/4$, in which the distance between vortices in the pair decreases and the direction of the pair rotates clockwise. In this case, the vortex pair is elongated, and asymmetric deformation occurs as shown by the result of the vortex method in Fig. 11(b). Thereafter, the vortex pair is broken up as shown in Fig. 11(c). Figure 12 shows the centroid position $|x_d|$ as a function of time. The centroid position of the moment model has remarkable error after the asymmetric deformation at $t = 2$, because the self-propelling speed u_{self} given by Eq. (14) is introduced on the assumption of a symmetric vortex pair. In our test calculations including the above result, the asymmetric deformation of the vortex pair is caused only when $a(t) < a_0(=C_0 R)$. For such asymmetric deformation, the moment model is not applicable.

The moment model itself does not have information on internal deformation of the vortex pair, while it gives the value of $a(t)/(C_0 R)$. Therefore, it is probably appropriate to regard $a(t) \geq C_0 R$ as the range of application of the moment model in linear background flows. Although there are applicable cases for $a(t) < C_0 R$, as shown in Fig. 7, it is difficult to distinguish such cases only by the results of the moment model. It is noteworthy that the length scale and the dipole moment obtained by the moment model are always in good

agreement with those obtained by the vortex method even in the case of the broken vortex pair, because the background flow is linear in this subsection.

In this section, results of typical cases in which the initial self-propelling speed of the vortex pair u_{self} is in the same range of the background flow U are shown. In case of $u_{\text{self}} \gg U$, u_{self} plays a dominant role in translation of the vortex pair, but qualitative property of rotation, length scale evolution, and deformation of the vortex pair in the linear background flows are the same as in the case of $u_{\text{self}} \sim U$. On the other hand, the vortex pair is passively advected by the background flow in case of $u_{\text{self}} \ll U$. In this case, the moment model is applicable for a long time because the linear background flow (20) itself is symmetric. Nevertheless, it seems meaningless to apply the moment model to the vortex pair with extremely large deformation even if the vortex pair is symmetric.

In order to extend the moment model for the vortex pair in asymmetric deformation, as shown in Figs. 11 and 16, the introduction of the second- or higher-order moment of vorticity is promising. In another instance, the introduction of an additional number of dipole elements is also promising.

C. Motion of a vortex pair in a weakly nonlinear background flow

Let us consider a flow field induced by a point vortex at the origin as a background flow,

$$\Psi = -\frac{B}{2}\log(x^2 + y^2). \tag{29}$$

Space derivatives of the velocity of the above background flow depend on the position, in other words the velocity is not a linear function of x and y. Such a background flow is called "nonlinear" here. The second-order terms of the Taylor series of Eq. (29) are equivalent to a strain flow. The value of nth-order terms is approximately proportional to $(a/|x_d|)^n$. The nonlinear effect on the moment model comes from these third- and higher-order terms of the Taylor series. In this subsection, a weakly nonlinear case for $a < |x_d|$ is calculated. The strength $B = 2/\pi$ is used for calculation. Initial conditions of the vortex pair are set to $x_d = (2,0)$, $a_0 = 0.4599(R = 0.5)$, $\mu = \sqrt{2}/5$, and $\beta = \pi/3$ or $-\pi/3$.
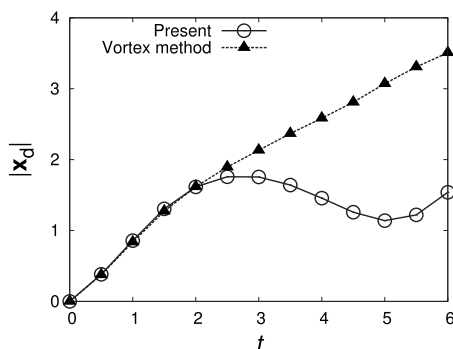

FIG. 12. Position of the vortex pair centroid in the shear flow displayed in Fig. 11. The centroid is calculated by the moment model and the vortex method.
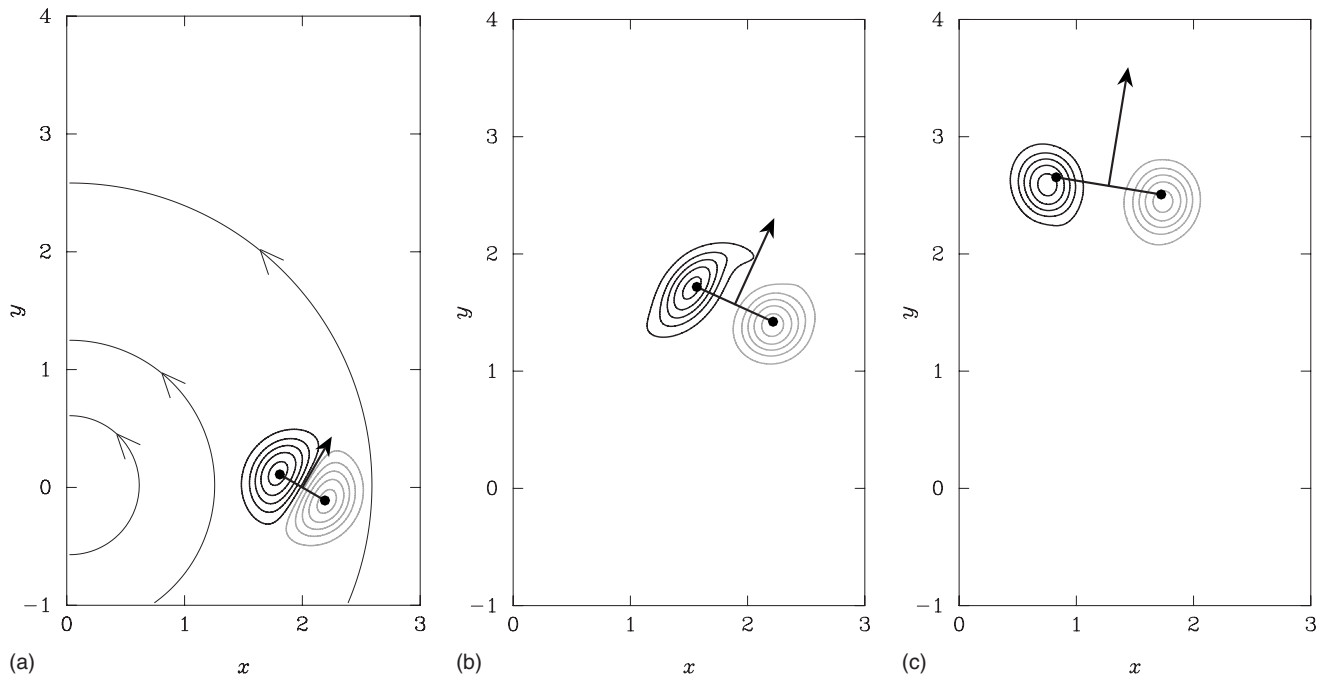
FIG. 13. Evolution of a vortex pair in the weakly nonlinear background flow $\Psi=-(1/\pi)\log(x^2+y^2)$ for the initial conditions $\boldsymbol{x}_d=(2,0)$, $\mu=\sqrt{2}/5$, $\beta_0=\pi/3$, and $a_0=0.4599(R=0.5)$. Streamlines of the background flow are also shown in (a). (a) $t=0$, (b) $t=4$, and (c) $t=8$.

Figure 13 illustrates results of the moment model and the vortex method in the case of a separated and rotated vortex pair similar to the cases of Table I [(3) and (6)] except the rotation direction. The result of the vortex method shows that the shape of each vortex gradually approaches a circle [see Fig. 13(c)]. The movement of the vortex pair is well repre-sented by the moment model, as shown in Fig. 13, which is similar to Fig. 9. Profiles of the centroid position plotted in Fig. 14 show a good agreement between the moment model and the vortex method even in this weakly nonlinear back-ground flow. Profiles of the length scale are also plotted in Fig. 15. There is a slight error in Fig. 15 due to the slight deviation of $\boldsymbol{x}_d$ and the truncation of second- and higher-order terms in Eq. (17). The moment model sufficiently well represents the behavior of the vortex pair in this case.

Finally, Fig. 16 shows evolution of the vortex pair in the case of that the distance between two vortices decreases and the direction of the vortex pair rotates. This behavior is simi-lar to the cases of Table I [(1) and (4)]. It is observed from vorticity contours obtained by the vortex method that the distance between vortices in the pair is reduced and the nega-tive vortex is elongated by the background flow [see Fig. 16(b)]. The centroid of the moment model disagrees with that of the vortex method at $t=4$, when the further asymmet-
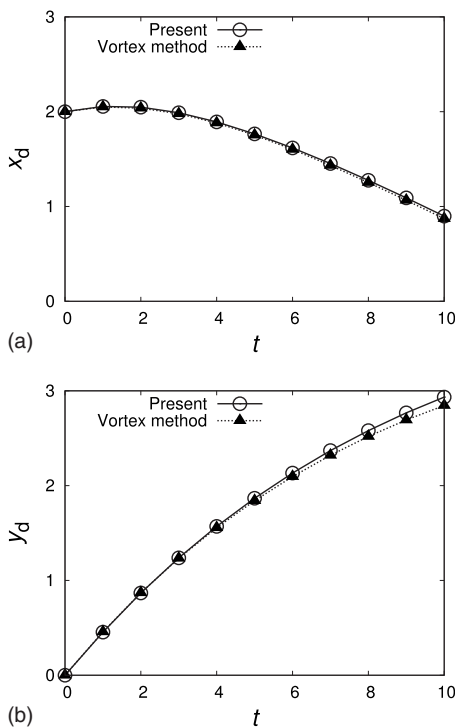

FIG. 14. Position of the centroid of the vortex pair in the weakly nonlinear background flow shown in Fig. 13. The centroid is calculated by the moment model and the vortex method.
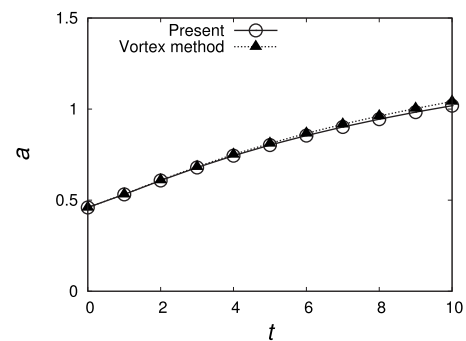

FIG. 15. Length scale of the vortex pair in the weakly nonlinear background flow shown in Fig. 13. The length scale is calculated by the moment model and the vortex method.
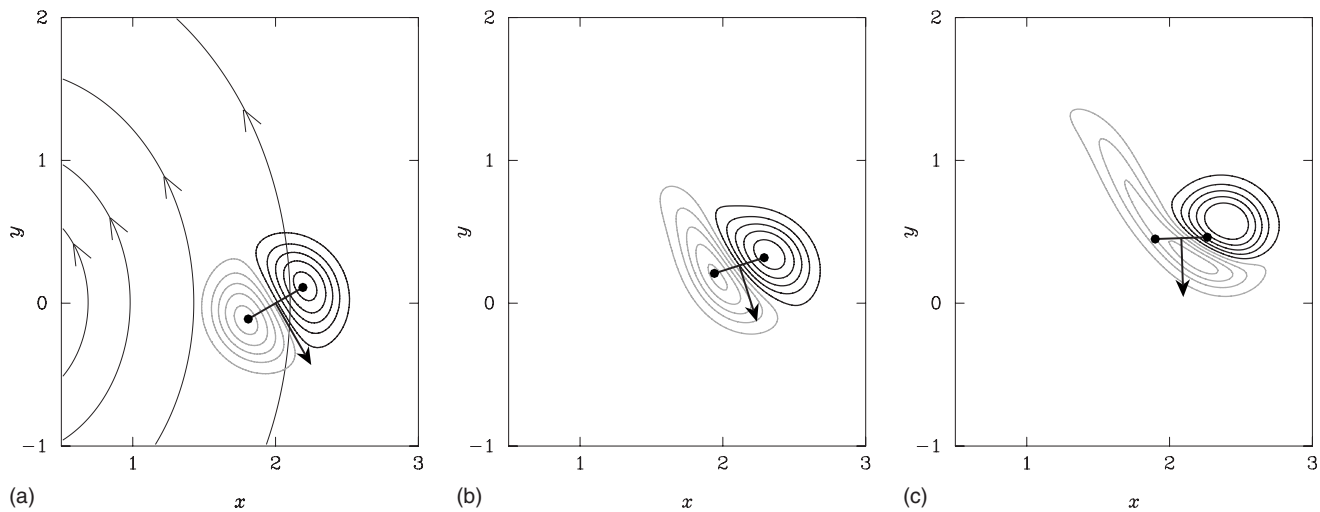
FIG. 16. Evolution of a vortex pair in the weakly nonlinear background flow $\Psi=-(1/\pi)\log(x^2+y^2)$ for the initial conditions $x_d=(2,0)$, $\mu=\sqrt{2}/5$, $\beta_0=-\pi/3$, and $a_0=0.4599(R=0.5)$. (a) $t=0$, (b) $t=2$, and (c) $t=4$.

ric deformation is observed. This result indicates that the moment model is not applicable to this asymmetrically deformed vortex pair, as has been already shown in Fig. 11.

VI. CONCLUSION

In the present paper, a moment model for evolution of a vortex pair in steady background flows was presented. A vortex pair is modeled by three time-dependent variables and two invariants: the centroid position $x_d(t)$, the dipole moment $\mu(t)$, and the length scale $a(t)$ are the variables, and the circulation Γ and the area S of the vortex pair are the invariants. The evolution of the vortex pair is described by a set of ordinary differential equations for these three variables. The length scale a is introduced as the distance between two vortices in the pair and the proportional relation between the length scale a and the magnitude of the dipole moment μ is obtained from Kelvin's circulation theorem. The self-propelling speed of the pair u_{self} is also introduced in response to a wide range of the length scale. The equation for the dipole moment μ is derived from conservation of momentum.

The dipole moment μ and the length scale a of the moment model are exact when a background flow U is a linear function of the coordinates x and y. Therefore, the validity of the moment model in the linear background flows eventually depends on the modeling of u_{self}. Numerical results show that the centroid position x_d calculated by u_{self} introduced in Eq. (14) is in good agreement with the centroid of the actual vortex pair in comparison with cases using u_{self} given by Eq. (12) and (13), if the vortex pair is symmetric.

When vortices in the pair are separated by the linear background flows, the shape of each vortex approaches a circle and the symmetry of the vortex pair is preserved as far as our calculations show. In such cases for $a>C_0R$, u_{self} (14)

gives sufficiently good approximation to the motion of the separated vortex pair. On the other hand, there is a possibility that the actual vortex pair asymmetrically deforms when $a<C_0R$. The moment model is not applicable to such a deformed vortex pair because the asymmetric deformation is not considered in derivation of u_{self}.

The motion of a vortex pair in a weakly nonlinear background flow was also calculated by the moment model. In our calculations, behavior of the vortex pair and the range of application of the moment model are qualitatively the same as the case of linear background flows.

APPENDIX: DIPOLE MOMENT FOR LINEAR BACKGROUND FLOWS

Exact solutions of Eqs. (19) for the linear background flow (20) are given in this Appendix. If $A=0$ the dipole moment is

$$\mu_x(t)=\mu_{x0},$$
$$\mu_y(t)=\mu_{y0}-\mu_{x0}t, \tag{A1}$$

where $(\mu_{x0},\mu_{y0})=(\mu_x,\mu_y)|_{t=0}$. The solutions of Eq. (19) for $A>0$ is obtained as

$$\mu_x(t)=\mu_{x0}\cos\sqrt{A}t+\sqrt{A}\ \mu_{y0}\sin\sqrt{A}t,$$
$$\tag{A2}$$
$$\mu_y(t)=\mu_{y0}\cos\sqrt{A}t-\frac{1}{\sqrt{A}}\mu_{x0}\sin\sqrt{A}t.$$

Both $\mu_x(t)$ and $\mu_y(t)$ are sinusoidal functions of time with a period $2\pi/\sqrt{A}$. The dipole moment obtained by solving Eq. (19) for $A<0$ is

$$\mu_x(t) = \left(\frac{1}{2}\mu_{x0} - \frac{\sqrt{|A|}}{2}\mu_{y0}\right)e^{\sqrt{|A|}t}$$

$$+ \left(\frac{1}{2}\mu_{x0} + \frac{\sqrt{|A|}}{2}\mu_{y0}\right)e^{-\sqrt{|A|}t},$$

$$\text{(A3)}$$

$$\mu_y(t) = \left(\frac{1}{2}\mu_{y0} - \frac{1}{2\sqrt{|A|}}\mu_{x0}\right)e^{\sqrt{|A|}t}$$

$$+ \left(\frac{1}{2}\mu_{y0} + \frac{1}{2\sqrt{|A|}}\mu_{x0}\right)e^{-\sqrt{|A|}t}.$$

These solutions are independent of the position x_d.

[1] K. Haines and J. Marshall, "Eddy-forced coherent structures as a prototype of atmospheric blocking," Q. J. R. Meteorol. Soc. **113**, 681 (1987).

[2] K. Ahlnäs, T. C. Royer, and T. H. George, "Multiple dipole eddies in the Alaska coastal current detected with landsat thematic mapper data," J. Geophys. Res. **92**, 13041, DOI: 10.1029/JC092iC12p13041 (1987).

[3] S. Kida, M. Takaoka, and F. Hussain, "Formation of head-tail structure in a two-dimensional uniform straining flow," Phys. Fluids A **3**, 2688 (1991).

[4] R. R. Trieling, J. M. A. van Wesenbeeck, and G. J. F. van Heijst, "Dipolar vortices in a strain flow," Phys. Fluids **10**, 144 (1998).

[5] D. D. Hobson, "A point vortex dipole model of an isolated modon," Phys. Fluids A **3**, 3027 (1991).

[6] B. K. Shivamoggi and G. J. F. van Heijst, "Generalized point-vortex model for the motion of a dipole-vortex on the β-plane," Fluid Dyn. Res. **23**, 113 (1998).

[7] M. V. Melander, N. J. Zabusky, and A. S. Styczek, "A moment model for vortex interactions of the two-dimensional Euler equations. Part 1. Computational validation of a Hamiltonian elliptical representation," J. Fluid Mech. **167**, 95 (1986).

[8] P. G. Saffman, *Vortex Dynamics* (Cambridge University Press, Cambridge, 1992).

[9] H. Lamb, *Hydrodynamics*, 6th ed. (Dover, New York, 1945).

[10] G. S. Winckelmans, "Topics in vortex methods for the computation of three- and two-dimensional incompressible flows," Ph. D. thesis, California Institute of Technology, 1989.

[11] P. H. Roberts, "A Hamiltonian theory for weakly interacting vortices," Mathematika **19**, 169 (1972).

[12] T. F. Buttke, "Velicity methods: Lagrangian numerical methods which preserve the Hamiltonian structure of incompressible fluid flow," in *Vortex Flows and Related Numerical Methods*, NATO Advanced Studies Institute, Series C: Mathematical and Physical Sciences Vol. 395, edited by J. T. Beale, G. H. Cottet, and S. Huberson (Kluwer Academic, Dordrecht, 1993) p. 39.

[13] G. H. Cottet and P. D. Koumoutsakos, *Vortex Methods: Theory and Practice* (Cambridge University Press, Cambridge, 2000).

[14] V. V. Meleshko and G. J. F. van Heijst, "On Chaplygin's investigations of two-dimensional vortex structures in an inviscid fluid," J. Fluid Mech. **272**, 157 (1994).